AIP | Journal of Applied Physics

Field-emission properties of individual GaN nanowires grown by chemical vapor deposition

Yongho Choi, Mario Michan, Jason L. Johnson, Ali Kashefian Naieni, Ant Ural et al.

Citation: J. Appl. Phys. **111**, 044308 (2012); doi: 10.1063/1.3685903
View online: http://dx.doi.org/10.1063/1.3685903
View Table of Contents: http://jap.aip.org/resource/1/JAPIAU/v111/i4
Published by the American Institute of Physics.

Field-emission properties of individual GaN nanowires grown by chemical vapor deposition

Yongho Choi,[1,a)] Mario Michan,[1] Jason L. Johnson,[2] Ali Kashefian Naieni,[1] Ant Ural,[2] and Alireza Nojeh[1,b)]
[1]*Department of Electrical and Computer Engineering, University of British Columbia, Vancouver, British Columbia, V6T 1Z4, Canada*
[2]*Department of Electrical and Computer Engineering, University of Florida, Gainesville, Florida 32611, USA*

(Received 22 March 2011; accepted 16 January 2012; published online 22 February 2012)

Single crystalline GaN nanowires were synthesized using chemical vapor deposition. Devices containing individual GaN nanowires were fabricated using contact printing. The local turn-on electric field at the tip of the GaN nanowires was compared to that of other nanomaterials. The quality of contact between GaN nanowires and metal electrodes was found to affect the field-emission behavior significantly. It was also observed that the field-emission behavior of individual GaN nanowires follows the conventional Fowler-Nordheim model in the range of applied electric fields. © *2012 American Institute of Physics*. [doi:10.1063/1.3685903]

INTRODUCTION

When a strong electric field is applied to a material, electrons are extracted from the surface by quantum mechanical tunneling through the vacuum energy barrier. This phenomenon is known as field-emission[1] and is attractive for electron source applications because of high brightness, low energy spread, good energy efficiency and fast response. The performance of an electron-beam system is strongly affected by the properties of its electron emitter. Thus, great attention has been dedicated to finding field-emitters with high performance and reliability.

GaN is a direct bandgap semiconductor (~3.4 eV) with high melting point and carrier mobility, strong chemical stability and high electric breakdown field. Because of these excellent properties, it has broad applications in light emitting diodes,[2,3] laser diodes,[4] photodetectors,[5] field-effect transistors[6] and high-temperature and high-power-density electronics.[7,8] Moreover, GaN nanowires, which are quasi-one-dimensional structures of GaN, are interesting candidates for field-emitters because of their low electron affinity (2.7–3.3 eV)[9,10] and high-aspect-ratio geometry. Previous studies on field-emission properties of GaN nanowires have focused on collections of these nanowires.[11–16] It has been observed that GaN bundles have lower turn-on field and higher emission current density compared to bulk GaN and relatively longer lifetime and better stability than some of the other nanomaterials.[12] However, to the best of our knowledge, the field-emission properties of individual GaN nanowires have not been studied so far. Such studies are important in order to gain a better understanding of their field-emission behavior and be able to engineer field-emitters based on them.

We synthesized GaN nanowires using chemical vapor deposition. Devices containing individual GaN nanowires were fabricated using the contact printing technique. The field-emission properties were investigated for a variety of device configurations and contact electrode materials. In this paper we discuss the fabrication and field-emission experiments and attempt to shed further light on the emission behavior.

FABRICATION AND EXPERIMENTS

A 500-nm-thick SiO_2 layer was thermally grown on a Si (100) substrate and a layer of gold approximately 2 nm thick was deposited as catalyst using electron-beam evaporation. The sample was placed in a quartz-tube furnace (with a diameter of 1 in.) and a gallium metal source was placed approximately 3 cm upstream of the sample. The temperature was ramped up to 850 °C, and a flow of 500 sccm of Ar was maintained during heating and a subsequent 15 min of annealing. For the nucleation of the GaN nanowires, 13 sccm of NH_3 and 300 sccm of H_2 were introduced into the reaction chamber for 5 h. Finally, the furnace was allowed to cool down to room temperature under a flow of 300 sccm of H_2 before removing the sample. Based on scanning electron microscopy (SEM) and transmission electron microscopy (TEM), the GaN nanowires were found to have diameters from 15 to 60 nm and lengths from 1 to 10 μm (Fig. 1). The GaN nanowires had a single crystalline Wurtzite structure, as determined by selected area diffraction and x-ray diffraction using a transmission electron microscope. Photoluminescence analysis showed that the nanowires had a ~3.4 eV energy bandgap. More detail on the growth and characterization steps can be found in Refs. 17 and 18.

Since the as-grown GaN nanowires were highly dense and randomly oriented, they needed to be partially transferred and aligned to make devices containing individual GaN nanowires. For this, the contact printing method was used[19] [Fig. 2(a)]. The sample containing the GaN nanowires was inverted and rubbed on the target substrate at a constant speed of 20 μm/s. A constant force was applied by attaching a 7-g weight to the back of the sample. Because of the high density of nanowires on the as-grown substrate, multiple

[a)]Present address: Department of Energy Resources Engineering, Jungwon University, Goesangun, Chungcheongbukdo, 367-805, Korea.
[b)]Author to whom correspondence should be addressed. Electronic address: anojeh@ece.ubc.ca.

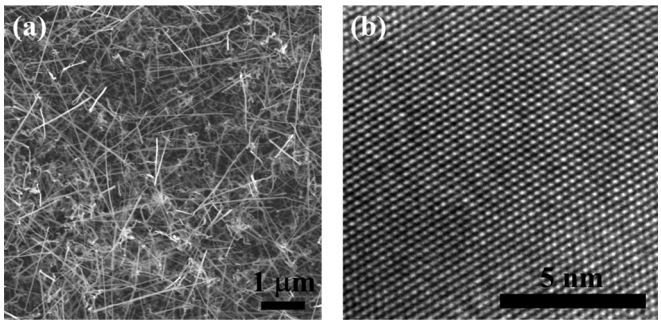

FIG. 1. (a) SEM image of as-grown GaN nanowires. (b) TEM image of an individual GaN nanowire showing its single crystalline structure. The diameters of the nanowires were found to be in the range of 15–60 nm.

printing steps were needed to progressively reduce the density of nanowires on the target substrate: Most of the nanowires were transferred onto dummy substrates by the first few printing steps [Fig. 2(b)]. Eventually, the as-grown sample was left with a suitably low density for transfer to the final target substrate [Fig. 2(c)].

Two main types of devices were fabricated to investigate the effect of the proximity of the nanowire to the substrate: those where the nanowires rest on the oxide surface or are very close to it, Type-1 [Fig. 3(a), electrode over nanowire] and Type-3 [Fig. 3(c), nanowire over electrode], and those with the nanowires suspended over a trench, forming a cantilever-like structure, Type-2 [Fig. 3(b)]. The patterned electrode opposing the nanowire served as anode in the experiments, eliminating the need for an external anode and allowing us to know the cathode-anode distance precisely in each case.

In all the devices, the metal electrodes were patterned using photolithography, electron beam evaporation, and lift-off. For the cantilever-type devices, a section of the SiO_2 substrate was removed using a buffered oxide etch solution

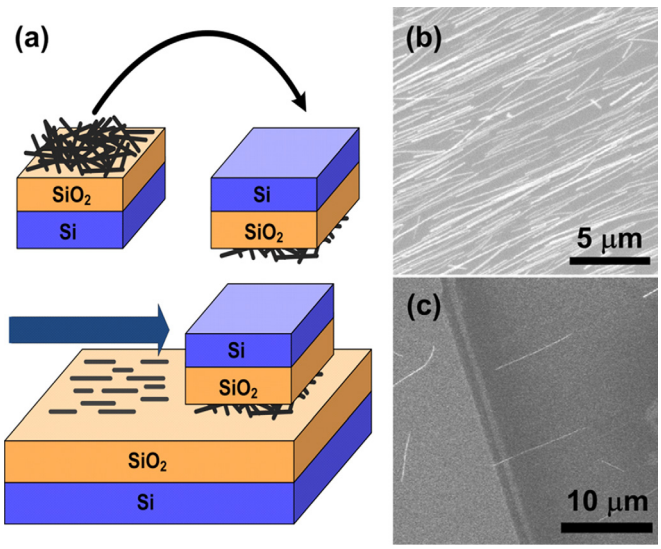

FIG. 2. (Color online) (a) Schematic representation of the contact printing method. The source substrate containing GaN nanowires was moved on the target substrate with a constant speed of ~20 μm/s and constant force (7-g weight on the back side of source substrate). (b) and (c) SEM images showing the transferred and well-aligned GaN nanowires on substrates with high and low density, respectively.

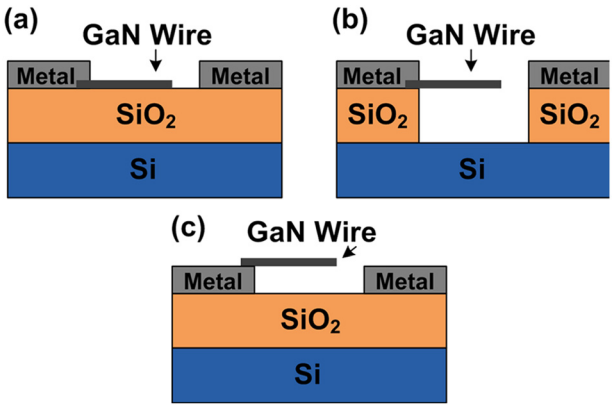

FIG. 3. (Color online) Cross-sectional schematic of the fabricated devices. (a) Electrode on top of the end of nanowire lying on substrate, Type-1. (b) Similar to (a), but oxide etched from underneath the nanowire to form a free-standing, cantilever-like structure, Type-2. (c) Nanowire end on top of the electrode, Type-3. In Type-3 devices, depending on its length, the nanowire either did or did not touch the oxide surface.

in order to form the trench. Ohmic contact was achieved by depositing four metal layers from bottom to top: Ti (20 nm), Al (80 nm), Pt (40 nm), and Au (100 nm) (both devices Type-1 and Type-2 were made with Ohmic contacts).[20] Type-3 devices were made with two different electrode materials, Mo (50 nm) or a double-layer of Cr (20 nm)/Pd (50 nm). The field-emission experiments were carried out at $10^{-4} - 10^{-5}$ Torr at room temperature and emission currents were measured using a Keithley 6517 A electrometer, which also served to apply the bias voltage. A scanning electron micrograph of a typical device (Type-2) is shown in Fig. 4.

RESULTS AND DISCUSSION

Figures 5(a) and 5(b) show the emission current from a nanowire cantilever and a nanowire lying on the oxide surface, Type-2 and Type-1, respectively, versus applied electric field (both are for devices with Ohmic-contact electrodes). The distances between the electrodes were 11.4 and 3.4 μm, and the distances from the tip of the GaN nanowire to the anode were 7 and 1.8 μm for the Type-2 and Type-1 devices, respectively. The maximum current obtained from each nanowire was a few tens of nanoAmps before the device was permanently damaged under an

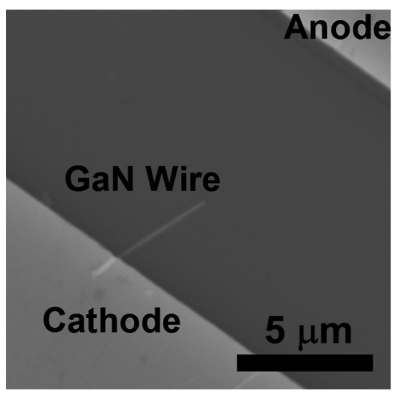

FIG. 4. SEM image of a fabricated device with an individual GaN nanowire.

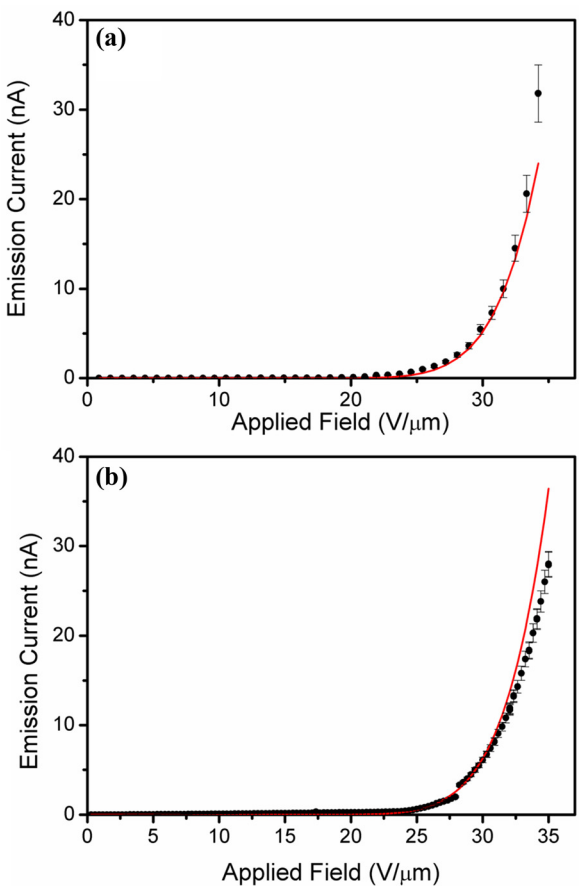

FIG. 5. (Color online) Emission current vs macroscopic (applied) electric field. The dots are the experimental data and the lines represent the emission current calculated using the Fowler-Nordheim (F-N) equation with a GaN work function of 4.1 eV and the field enhancement factor extracted from experimental data. Figures (a) and (b) are for Type-2 and Type-1 devices, respectively.

applied electric field greater than 35 V/μm. The discontinuity in the field-emission current seen on Fig. 5(b) was not observed in other tested devices. Therefore, we believe that it is not a fundamental property of the nanowire. Instead, it could be the result of a side effect such as change in the quality of the contact between the nanowire and the electrode due to local Joule heating.

The field-emission current from a metallic surface can be calculated using the Fowler-Nordheim (F-N) cold field-emission theory[1] through the equation[21]

$$J = {t_F}^{-2} \cdot a \cdot \phi^{-1} \cdot F^2 \cdot \exp\left(\frac{-v_F \cdot b \cdot \phi^{3/2}}{F}\right), \qquad (1)$$

which can also be written in the form

$$\ln\left(\frac{J}{V^2}\right) = \left[\frac{-v_F \cdot b \cdot \phi^{3/2} \cdot d}{\beta}\right] \cdot \frac{1}{V} + \ln\left(\frac{{t_F}^{-2} \cdot a \cdot \phi^{-1} \cdot \beta^2}{d^2}\right), \qquad (2)$$

where F is the local electric field (V/m) at the barrier, J is the current density (A/m^2), ϕ is the work function (eV), d is the anode-cathode distance (m), V is the applied voltage and a and b are constants with values of 1.541434×10^{-6} A eV V^{-2} and 6.830890 eV$^{-3/2}$ V nm^{-1}, respectively. v_F and t_F are the field-emission elliptic functions and can be written as $v_F(y) \approx 1 - y^2 + (1/3) \cdot y^2 \cdot \ln y$ and $t_F(y) \approx 1 + (1/9)[y^2 - y^2 \cdot \ln y]$, where $y = c \cdot F^{1/2}/\phi$ and c is a constant with the value of 1.199985 eV V$^{-1/2}$ nm$^{1/2}$. The field enhancement factor, β, is the ratio of the local electric field at the nanowire tip and the applied electric field (applied voltage divided by the separation of electrodes).

Figure 6 shows the data (dots) of Fig. 5 plotted on ln (J/V^2) versus $1/V$ axes — the so-called F-N plot. Only the points where measurable field-emission current exists are shown on the figure. As can be seen from Eq. (2), the field enhancement factor, β, can be extracted from the experimental data using the ln (J/V^2) versus $1/V$ relationship. Using a workfunction value of 4.1 eV for GaN, the calculated field enhancement factors of the individual GaN nanowires are 170 and 167 for the Type-2 and Type-1 device, respectively. The solid lines in Figs. 5 and 6 represent our fits using these field enhancement factors in the F-N Eq. (1). We assumed the diameter of this particular nanowire to be 50 nm based on SEM imaging, although this is an approximation due to the resolution limit of our SEM. However, following the results of Ref. 22, around this value of diameter, we expect the field enhancement factor not to be as sensitive to diameter as it is for smaller diameters. Therefore, using an approximate value for the diameter is reasonable. We also conducted electrostatic simulations (using the software package COMSOL Multiphysics) in order to compare with the experimental value of the field enhancement factor.[23] Using the device geometry and dimensions described above and 50 nm for the nanowire diameter, the simulation yielded a field enhancement factor of 163 for the Type-2 device, in excellent agreement with the experimental estimate.

An important question in experiments on individual nanowires is whether the emission is truly due to the nanowire or from its surrounding structures such as the metal

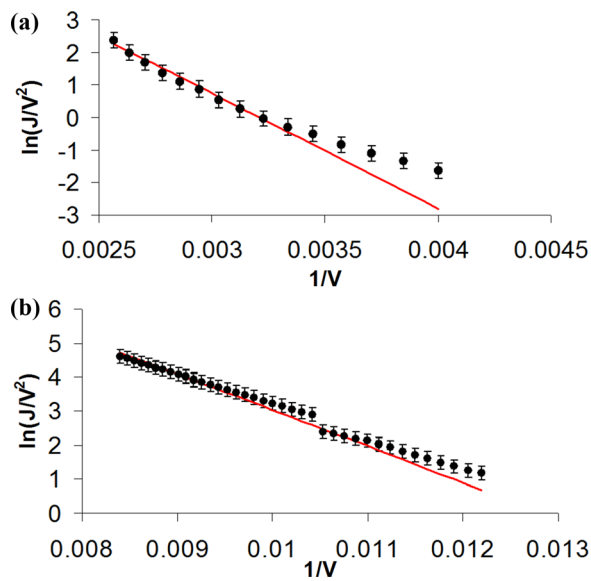

FIG. 6. (Color online) The emission current density data of Fig. 5 plotted on F-N axes [ln (J/V^2) vs $1/V$] for Type-2 (a) and Type-1 (b) devices. The dots are the experimental data and the lines are our straight-line fit.

electrodes. To investigate this, we calculated the field enhancement factor assuming that emission had happened from the electrode, that is using the slope of the line in Fig. 6(a) and the work function of Au, 5.1 eV, which constituted the top layer of the electrodes. This led to a calculated field enhancement factor of 227, which is greater than the value of 170 calculated using the 4.1 eV work function of GaN. However, this is not reasonable because the electrode, having a larger surface area than the nanowires and not the same high-aspect-ratio geometry, should have resulted in smaller field enhancement. This is equivalent to saying that GaN nanowires have both lower workfunction and sharper geometry compared to the electrodes and, therefore, it is unlikely that the electrodes would make a significant contribution to the emission current. To further investigate this point, field-emission experiments were conducted using devices that only contained electrodes and no GaN nanowires. Using the slope of the obtained F-N plot and the Au work function, the field enhancement factor was calculated to be 106 based on the experimental data – significantly smaller than that of devices containing nanowires, as expected.

The turn-on field for a collection of GaN nanowires has typically been defined as the field required for generating emission current densities of 0.01 mA/cm^2.[11,13,15,16] For an individual nanowire with a diameter of a few tens of nanometers, these would correspond to a current on the order of 10^{-16} A, which is below the resolution of our measurement circuitry. In our devices, the first noticeable sign of turn-on was observed at an applied field of ~21 V/μm (at which the current was ~100 pA). This field is greater than that for collections of GaN nanowires (which is typically less than 10 V/μm). On the other hand, it is not really appropriate to compare our devices to those including many nanowires, as they have widely different geometries and effects such as screening are also present in collections. Instead, it is more meaningful to compare the local turn-on field of our devices (at the nanowire tip) to that of other individual nanowires.

It has been observed that β is linearly proportional to the separation of electrodes, d.[22] Therefore, for a given applied electric field, a shorter distance between the electrodes means a lower local electric field at the tip of the nanowire. In order to compare the turn-on fields of the devices with different electrode separations, local electric fields were calculated using the experimental value of β obtained above. The local turn-on electric field was $\sim 3.7 \times 10^3$ V/μm for our Type-2 device. In other experiments, the local turn-on electric fields can be calculated as $\sim 2.8 \times 10^3$ V/μm at the emission current of 1 pA for individual B nanowires, $\sim 5 \times 10^3$ V/μm at the emission current of 10 nA for individual Bi_2S_3 nanowires, and $\sim 9 \times 10^3$ V/μm at the emission current of 100 nA for individual ZnO nanowires.[24–26] Although the values of the currents measured at turn-on were different in these experiments (which could, for instance, be due to the different sensitivities of the various measurement setups, among other factors), these values are all in the range of a V/nm, which is the typical field required for quantum mechanical tunneling. As it can be seen, our GaN nanowires perform similarly to other nanowires in this regard. Furthermore, the local turn-on electric field for a collection of GaN nanowires was calculated as $\sim 4.1 \times 10^3$ V/μm, which is again comparable to the value we obtained for an individual GaN nanowire, although the macroscopic turn-on fields were quite different in the two cases.[16] Consequently, it seems that the comparison of local electric fields calculated using the applied field and β is more appropriate than the comparison of the applied (macroscopic) electric field or the comparison of β itself among different nanowires and in different experiments.

Field-emission theory for semiconducting materials predicts a nonlinear behavior for the emission current.[27] At low electric fields, the emission current is determined by the tunneling probability and the field-emission behavior of the semiconductor is similar to that of metals. At medium electric fields, the emission current becomes saturated due to insufficient carrier supply. In this regime, the emission current is greatly affected by the energy band structure of the semiconducting material. In addition, as the applied field and the resulting emission current increase, the resistance of the emitter (including bulk and contact resistance) and space-charge effects among the emitted electrons also contribute to current saturation. At high electric fields, the emission current rapidly increases due to the field penetration into the depletion region, which results in a greatly increased number of carriers.

The saturation and subsequent rapid increase of the emission current were not observed in our experiments, in contrast with what has been observed for other semiconducting nanomaterials.[28–31] In fact, increasing the field further in our experiments led to the destruction of the devices and we were not able to observe a possible saturation regime or beyond. As shown in Fig. 5, the measured emission current followed the F-N theory reasonably well, although a gradual deviation was observed as the field became stronger.

We also investigated Schottky-contact devices, Type-3. Interestingly, no emission current was observed from either the Mo- or the Cr/Pd-electrode devices. Based on our preliminary studies, our GaN nanowires are N-type, likely due to O_2 impurities and/or N vacancies, with an energy bandgap of approximately 3.4 eV.[18] Electrons in the metal electrode have to overcome the Schottky barrier, $\mathbf{\Phi}_{bn}$ (~0.8 eV for Mo electrode and ~1.2 eV for Cr/Pd electrode), in order to be injected into GaN.[32,33] It is expected that the major part of the externally applied voltage drops over a region around the nanowire tip, and thus the region around the metal-nanowire contact only experiences a small reverse bias (Fig. 7). Under these conditions, the field-emission current is limited by the Schottky contact barrier as insufficient electrons are transferred to the GaN nanowire. For instance, the reverse saturation current density through the Schottky barrier for Mo-electrode devices is approximately 1×10^{-5} mA/cm^2, calculated using thermionic emission theory for an ideal Schottky diode, $J_s = A^{**} \cdot T^2 \cdot \exp(-q \cdot \phi_b / k_b \cdot T)$, where A^{**} is the effective Richardson constant (26.4 A cm$^{-2} \cdot$K^{-2} for N-type GaN),[32] T is temperature, ϕ_b is the Schottky barrier height, q is the electron charge and k_b is the Boltzmann constant. An experimental value of 1.8×10^{-5} mA/cm^2 for the reverse leakage current density of GaN-nanorod diodes was

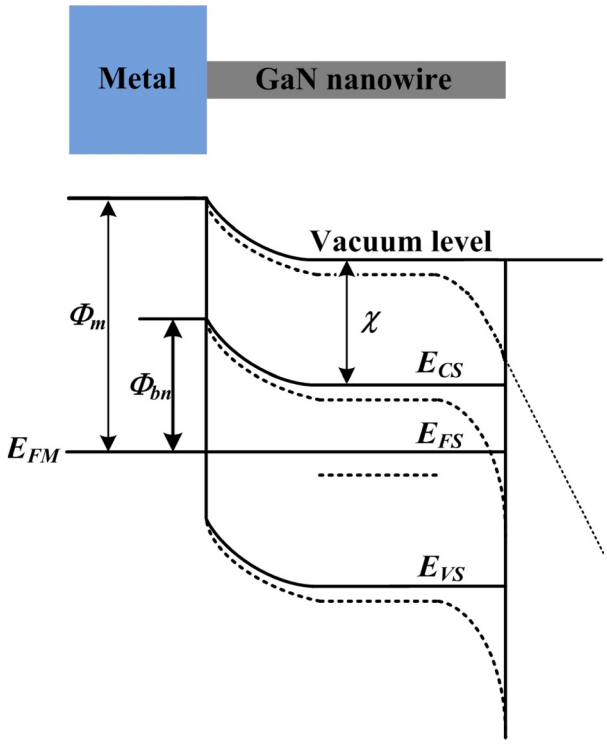

FIG. 7. (Color online) Qualitative representation of the energy band diagram of a GaN nanowire connected to a metal electrode and forming a Schottky contact. E_{FM} is the Fermi level of the metal, Φ_m is the workfunction of the metal and Φ_{bn} is the Schottky barrier height. E_{CS}, E_{FS}, E_{VS}, and χ are the conduction band edge, Fermi level, valence band edge, and electron affinity of the GaN nanowire, respectively. The Schottky barrier heights are ~0.8 eV for Mo electrodes and ~1.2 eV for Cr/Pd electrodes. The dotted lines are E_{CS}, E_{FS}, E_{VS} and vacuum level under field. Under applied bias, most of the potential drops around the nanowire tip and only a small reverse bias appears over the Schottky junction.

reported in Ref. 34. Therefore, our results show that the contact between the GaN nanowire and metal electrode plays an important role in field-emission behavior, and good Ohmic contact is desirable for sufficient electron supply and high emission current from the nanowire.

For the Type-1 device discussed previously, the field-emission current of ~300 pA was persistent for ~13 min, at which point the current dropped drastically and the device effectively turned off. Prior to this failure point, a slowly increasing trend in the field-emission current was observed, possibly due to Joule heating of the tip.[24] The device was investigated using SEM after the measurement and it was found that the failure was mainly due to the deformation of the metal electrode. It is known that a metal layer with nanoscale thickness has a high resistance, resulting in great Joule heating and electromigration problems.[35,36] For the same reason, it was difficult to obtain field-emission from all the devices we tested - most of the cathode electrodes were damaged before significant field-emission was observed. We also found that the contact area of the nanowire to the electrode was easily damaged in early stages of field-emission. These are important issues for nanostructured field-emitters and can be addressed by increasing the contact area between the nanowires and electrodes (by increasing the length of the section of the nanowire resting on or underneath the electrode), as well as using thicker cathode electrodes. Nonetheless, we observed that most of the nanowires were in their original positions after field-emission experiments, even for the devices where the nanowires had been placed over the electrodes. This shows that nanowires transferred by contact printing can have strong mechanical adhesion to the substrate.

CONCLUSION

By investigating two types of contacts (Ohmic and Schottky), we found that the field-emission behavior of individual GaN nanowires is greatly influenced by the contact conditions: good Ohmic contact is necessary to achieve high emission currents from GaN nanowires. A similar behavior would be expected for other nanowires. The local turn-on electric field was found to be similar to that of other nanomaterials. The field-emission behavior was fit to the Fowler-Nordheim model and the results show that the F-N equation is well suited for GaN nanowire field-emitters in relatively low applied electric fields.

ACKNOWLEDGMENTS

We thank Mu Chiao and Joshua Folk for access to wire-bonding facilities. We acknowledge financial support from the Natural Sciences and Engineering Research Council, the BCFRST Foundation/British Columbia Innovation Council, the Canada Foundation for Innovation and the British Columbia Knowledge Development Fund. AU acknowledges support from the Semiconductor Research Corporation. MM is grateful to the Bullitt Foundation for a graduate fellowship.

[1]R. H. Fowler and L. Nordheim, Proc. R. Soc. London, Ser. A **119**, 173 (1928)
[2]H. M. Kim, Y. H. Cho, H. Lee, S. I. Kim, S. R. Ryu, D. Y. Kim, T. W. Kang, and K. S. Chung, Nano Lett. **4**, 1059 (2004).
[3]F. Qian, S. Gradecak, Y. Li, C. Y. Wen, and C. M. Lieber, Nano Lett. **5**, 2287 (2005).
[4]S. Nakamura, S. Pearton, and G. Fasol, *The Blue Laser Diode: The Complete Story* (Springer-Verlag, Berlin, 2000).
[5]A. Osinsky, S. Gangopadhyay, R. Gaska, B. Williams, M. A. Khan, D. Kuksenkov, and H. Temkin, Appl. Phys. Lett. **71**, 2334 (1997).
[6]Y.-F. Wu, B. P. Keller, S. Keller, D. Kapolnek, P. Kozodoy, S. P. Denbaars, and U. K. Mishra, Appl. Phys. Lett. **69**, 1438 (1996).
[7]B. P. Luther, S. D. Wolter, and S. E. Mohney, Sens. Actuators B **56**, 164 (1999).
[8]W. Yi-Feng, D. Kapolnek, J. P. Ibbetson, P. Parikh, B. P. Keller, and U. K. Mishra, IEEE Trans. Electron Devices **48**, 586 (2001).
[9]R. J. Nemanich, P. K. Baumann, M. C. Benjamin, S. W. King, J. van der Weide, and R. F. Davis, Diamond Relat. Mater. **5**, 790 (1996).
[10]J. L. Shaw, H. F. Gray, K. L. Jensen, and T. M. Jung, J. Vac. Sci. Technol. B **14**, 2072 (1996).
[11]B. D. Liu, Y. Bando, C. C. Tang, F. F. Xu, J. Q. Hu, and D. Golberg, J. Phys. Chem. B **109**, 17082 (2005).
[12]B. Ha, S. H. Seo, J. H. Cho, C. S. Yoon, J. Yoo, G. C. Yi, C. Y. Park, and C. J. Lee, J. Phys. Chem. B **109**, 11095 (2005).
[13]D. K. T. Ng, M. H. Hong, L. S. Tan, Y. W. Zhu, and C. H. Sow, Nanotechnology **18**, 375707 (2007).
[14]C. T. Lin, G. H. Yu, X. Z. Wang, M. X. Cao, H. F. Lu, H. Gong, M. Qi, and A. Z. Li, J. Phys. Chem. C **112**, 18821 (2008).
[15]C. C. Chen, C. C. Yeh, C. H. Chen, M. Y. Yu, H. L. Liu, J. J. Wu, K. H. Chen, L. C. Chen, J. Y. Peng, and Y. F. Chen, J. Am. Chem. Soc. **123**, 2791 (2001).
[16]D. V. Dinh, S. M. Kang, J. H. Yang, S. W. Kim, and D. H. Yoon, J. Cryst. Growth **311**, 495 (2009).

[17]J. L. Johnson, Y. H. Choi, and A. Ural, J. Vac. Sci. Technol. B **26**, 1841 (2008).
[18]J. Johnson, Y. H. Choi, A. Ural, W. Lim, J. S. Wright, B. P. Gila, F. Ren, and S. J. Pearton, J. Electron. Mater. **38**, 490 (2009).
[19]Z. Y. Fan, J. C. Ho, Z. A. Jacobson, R. Yerushalmi, R. L. Alley, H. Razavi, and A. Javey, Nano Lett. **8**, 20 (2008).
[20]J. S. Wright, W. Lim, B. P. Gila, S. J. Pearton, J. L. Johnson, A. Ural, and F. Ren, Sens. Actuators B **140**, 196 (2009).
[21]R. G. Forbes, Appl. Phys. Lett. **89**, 113 (2006).
[22]Z. Xu, X. D. Bai, and E. G. Wang, Appl. Phys. Lett. **88**, 133107 (2006).
[23]COMSOL Multiphysics modeling and engineering simulation software, COMSOL AB, http://www.comsol.com/
[24]C. D. Zhang, J. M. Cai, M. Gao, H. L. Lu, Q. Zou, J. F. Tian, H. Hu, C. M. Shen, H. M. Guo, and H. J. Gao, Appl. Surf. Sci. **258**, 2149 (2011)
[25]Y. Yu, C. H. Jin, R. H. Wang, Q. Chen, and L. M. Peng, J. Phys. Chem. B **109**, 18772 (2005).
[26]Y. Huang, Y. Zhang, Y. Gu, X. Bai, J. Qi, Q. Liao, and J. Liu, J. Phys. Chem. C **111**, 9039 (2007).
[27]L. M. Baskin, O. I. Lvov, and G. N. Fursey, Phys. Status Solidi B **47**, 49 (1971).
[28]P. Yaghoobi, K. Walus, and A. Nojeh, Phys. Rev. B **80**, 115422 (2009).
[29]P. Yaghoobi, M. K. Alam, K. Walus, and A. Nojeh, Appl. Phys. Lett. **95**, 262102 (2009).
[30]J. R. Arthur, J. Appl. Phys. **36**, 3221 (1965).
[31]K. X. Liu, C. J. Chiang, and J. P. Heritage, J. Appl. Phys. **99**, 034502 (2006).
[32]V. R. Reddy, C. K. Ramesh, and C. J. Choi, Phys. Status Solidi A **203**, 622 (2006).
[33]L. Wang, M. I. Nathan, T. H. Lim, M. A. Khan, and Q. Chen, Appl. Phys. Lett. **68**, 1267 (1996).
[34]P. Deb, H. Kim, Y. X. Qin, R. Lahiji, M. Oliver, R. Reifenberger, and T. Sands, Nano Lett. **6**, 2893 (2006).
[35]G. Schindler, S. Penka, G. Steinlesberger, M. Traving, W. Steinhögl, and M. Engelhardt, Microelectron. Eng. **82**, 645 (2005).
[36]H. Yuejin and T. Cher Ming, *Nanoelectronics Conference, 2008, INEC 2008, 2nd IEEE International, 610* (INEC, Hong Kong, 2008).